

Photoluminescence emission in deep ultraviolet region from GaN/AlN asymmetric-coupled quantum wells

Guan Sun, Yujie J. Ding, Guangyu Liu, G. S. Huang, Hongping Zhao et al.

Citation: *Appl. Phys. Lett.* **97**, 021904 (2010); doi: 10.1063/1.3462324

View online: <http://dx.doi.org/10.1063/1.3462324>

View Table of Contents: <http://apl.aip.org/resource/1/APPLAB/v97/i2>

Published by the [American Institute of Physics](http://www.aip.org).

Related Articles

Photoreflectance study of direct-gap interband transitions in Ge/SiGe multiple quantum wells with Ge-rich barriers

Appl. Phys. Lett. **100**, 041905 (2012)

Effect of transverse electric field on helical edge states in a quantum spin-Hall system

Appl. Phys. Lett. **99**, 222111 (2011)

Long intersubband relaxation times in n-type germanium quantum wells

Appl. Phys. Lett. **99**, 201101 (2011)

Exciton confinement in homo- and heteroepitaxial ZnO/Zn_{1-x}Mg_xO quantum wells with $x < 0.1$

J. Appl. Phys. **110**, 093513 (2011)

InGaN/GaN quantum well structures with greatly enhanced performance on a-plane GaN grown using self-organized nano-masks

Appl. Phys. Lett. **99**, 181907 (2011)

Additional information on *Appl. Phys. Lett.*

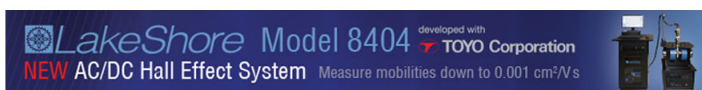
Journal Homepage: <http://apl.aip.org/>

Journal Information: http://apl.aip.org/about/about_the_journal

Top downloads: http://apl.aip.org/features/most_downloaded

Information for Authors: <http://apl.aip.org/authors>

ADVERTISEMENT



Photoluminescence emission in deep ultraviolet region from GaN/AlN asymmetric-coupled quantum wells

Guan Sun,¹ Yujie J. Ding,^{1,a)} Guangyu Liu,¹ G. S. Huang,¹ Hongping Zhao,¹ Nelson Tansu,¹ and Jacob B. Khurgin²

¹Department of Electrical and Computer Engineering, Lehigh University, Bethlehem, Pennsylvania 18015, USA

²Department of Electrical and Computer Engineering, Johns Hopkins University, Baltimore, Maryland 21218, USA

(Received 21 April 2010; accepted 18 June 2010; published online 12 July 2010)

We have investigated the photoluminescence spectra from GaN/AlN asymmetric-coupled quantum wells grown by metal-organic chemical vapor deposition. Deep ultraviolet photoluminescence peaks with photon energies up to 5.061 eV and dramatically improved intensities at low temperatures are identified due to recombination of electrons in the AlN coupling barrier with heavy holes in the GaN quantum wells. Photoluminescence quenching caused by relocation of photogenerated electrons under large internal electric fields, inherent in GaN/AlN asymmetric-coupled quantum wells, is observed. © 2010 American Institute of Physics. [doi:10.1063/1.3462324]

GaN/AlN heterostructures have promising applications in blue-violet light emitting and laser diodes, due to their wide band gaps.^{1,2} On the other hand, GaN/AlN quantum wells (QWs) and quantum dots (QDs) can be used to achieve high-speed intersubband (ISB) optoelectronic devices.^{3,4} GaN/AlN QWs are unique since extremely high internal electric fields approaching 10 MV/cm are present due to spontaneous and piezoelectric polarizations. Such large internal fields induce quantum confined Stark effect. Consequently, the overlap of electron and hole wave functions, transition energy and recombination rate of QWs are greatly reduced. Such a charge separation effect can be suppressed by a staggered structure.⁵ These strong internal fields can be exploited to enhance second-harmonic generation⁶ and quantum cascade detectors.⁷ However, when these QWs are grown on nonpolar planes,⁸ these internal electric fields vanish.

In this paper, we report our results on GaN/AlN asymmetric-coupled QWs. In the past, these heterostructures were primarily utilized in electroabsorption modulators and frequency doublers based on ISB transitions.⁹

Multiple GaN/AlN asymmetric-coupled QWs were grown in a low-pressure vertical VEECO P75 reactor with a high-speed rotation configuration. The reagents used during growth were ammonia, trimethylgallium, and trimethylaluminum. High-purity hydrogen and nitrogen were used as the carrier gases. All samples were grown on 2.5- μm -thick undoped (or n-) GaN templates grown on c-plane sapphire substrates. Each GaN template was grown at 1070 °C, which employed a 30-nm-thick GaN nucleation layer deposited at 515 °C with etch-back and recovery growth process.¹⁰ The active layers of the AlN/GaN/AlN asymmetric-coupled QWs consist of ten periods, see Table I. For comparison, two additional samples were grown, each of which consists of multiple single GaN/AlN QWs, see Table I. Both the AlN and GaN layers were grown at a temperature of 1070 °C, with growth rates being 3.6 nm/min and 4.5 nm/min, respectively.

Each sample has a 10-nm-thick GaN layer as the cap.

Photoluminescence (PL) spectra were measured by using a coherent 3 ps UV beam at 235 nm as the pump which is the third-harmonic output of a Ti:sapphire laser. The highest average pump power used in our experiment is 20 mW. Each sample of multiple GaN/AlN asymmetric-coupled QWs was mounted on a cold finger of a cryostat with its temperature being set in the range of 4.2–300 K. For the asymmetric-coupled QWs, we have identified two apparent transition peaks in the PL spectrum, see Fig. 1. For sample no. 1, the transition energies of the two peaks are 3.938 eV (P_{low}) and 5.061 eV (P_{high}), respectively, see Table I. When the widths of the two QWs are increased from 2 nm and 1.5 nm to 2.5 nm and 2 nm, respectively, the transition energies for the two peaks are reduced to 3.722 eV and 4.647 eV, respectively, due to the decreases in quantum-confinement energies. By decomposing each of the overall PL spectra into a linear superposition of the two transition peaks, we have deduced the ratio of the PL intensities for the higher- and lower-energy transition peaks to be 8.9 and 17 for sample nos. 1 and 2, respectively, which are anomalously large. Using NEXTNANO3 eight-band- $\mathbf{k}\cdot\mathbf{p}$ Schrödinger–Poisson solver,¹¹ we have plotted the energies of these states and their wave functions, see Fig. 2. One can see that the transition energies for $e_1\text{-}hh_1$ and $e_2\text{-}hh_2$ are both around 3.851 eV, which is

TABLE I. Characteristics for four samples are summarized. d_{AlN} and d_{GaN} stands for thicknesses of AlN and GaN layers, respectively; E_{low} stands for lower-energy transition peak (or the only peak) of asymmetric-coupled (or single) QWs, whereas E_{high} stands for higher-energy transition peak; I_{low} and I_{high} are integrated intensities of lower- and higher-energy transition peaks, respectively; FWHM is full width at half maximum; and R stands for ratio between PL intensities of the higher- and lower-energy transition peaks.

Sample	$d_{\text{AlN}}/d_{\text{GaN}}$ (nm)	E_{low} (FWHM) (eV)	E_{high} (FWHM) (eV)	I_{low} (a.u)	I_{high} (a.u)	R
1	4/2/1/1.5	3.938(0.308)	5.061(0.246)	11.3	101	8.9
2	4/2.5/1/2	3.722(0.285)	4.647(0.307)	7.3	121	16.6
3	4/1.5	4.335(0.263)	No peak	1	No peak	
4	4/2	4.145(0.350)	No peak	1.9	No peak	

^{a)}Tel.: (610) 758-4582. FAX: (610) 758-6279. Electronic mail: yud2@lehigh.edu.

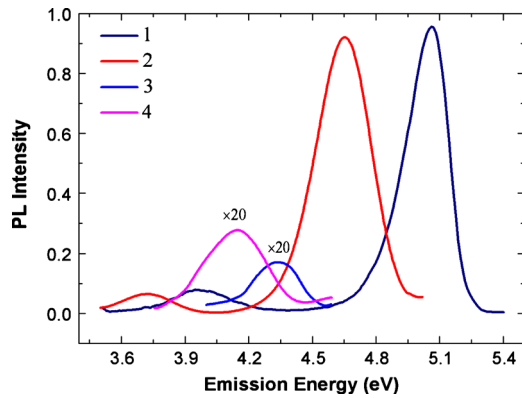


FIG. 1. (Color online) PL spectra measured at 4.2 K on different samples at pump power of 6 mW at 235 nm. The signals for sample nos. 3 and 4 are both multiplied by 20 for clarity.

very close to 3.938 eV deduced from Fig. 1. Since the full width at half maximum (FWHM) of peak at 3.938 eV is as high as 308 meV and the widths of two QWs only differ by 0.5 nm, transitions for e_1-hh_1 and e_2-hh_2 merged into one peak at 3.938 eV. However, the confined energy states within the coupled QWs for both sample nos. 1 and 2 do not support the higher-energy transition peaks at 5.061 and 4.647 eV, deduced from our experiment. Indeed, according to our calculations, these two energies are quite close to the transition energies for the electrons being localized inside the AlN coupling barrier and heavy holes at the two confined energy states in GaN QWs. Since the coupling barrier in the asymmetric-coupled QWs is rather thin, the overlap between the wave functions of the electrons inside the AlN coupling barrier and heavy holes inside the GaN QWs is large. Due to the presence of large built-in fields, the wave functions of the heavy holes have further penetrated into the AlN coupling barrier. As a result, the overlap between the wave functions of the electrons inside the AlN coupling barrier and heavy holes inside the GaN QWs has been further increased by the strong built-in fields. Thus, the signal of recombination of electrons inside AlN couple layer and holes in GaN wells could be stronger than that of electrons and holes in GaN QWs, which in fact is supported by our PL spectra. The ratio of P_{high} and P_{low} is even larger for sample no. 2. Such a result can be attributed to the fact that the wider QWs in sample no. 2 leads to a larger separation of electrons and holes inside the GaN QWs. This assumption is verified by our experimental

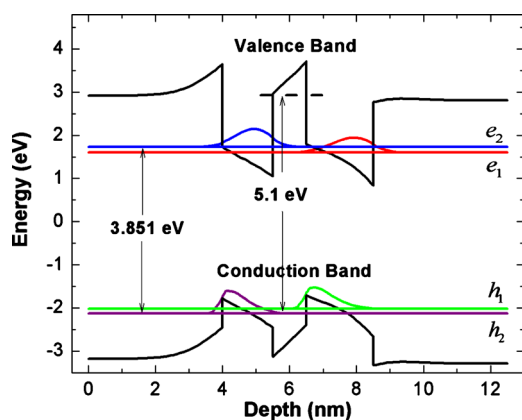


FIG. 2. (Color online) Typical band diagram of sample no. 1, calculated using NEXTRAN03 eight-band- $\mathbf{k} \cdot \mathbf{p}$ Schrödinger-Poisson solver.

result that the intensity of P_{low} in sample no. 2 is weaker than that for sample no. 1. Previously, recombination of the electrons inside an AlN wetting layer and heavy holes in the GaN quantum dot was used to explain the transition energy as high as 4.8 eV.¹² According to Fig. 1, each of the PL spectra for the single QWs consists of only a single peak at 4.335 eV and 4.145 eV for the two different well widths, respectively. These two energies are significantly higher than those for the lower-energy transition peaks in the asymmetric-coupled QWs. The higher energies are caused by the reduction in the quantum confinement by introducing the second QW in the asymmetric-coupled QWs and reduction in the coupling barrier width compared with the single QW. Moreover, based on Fig. 1, the PL intensities for the lower-energy transitions in the asymmetric-coupled QWs are stronger than those from the single QW by factors of 11 and 3.8, respectively. Furthermore, the PL intensities for the higher-energy transitions in the asymmetric-coupled QWs are higher than those from the single QW by factors as high as 101 and 63, respectively. Such huge enhancements are caused by the asymmetries of the coupled QWs, the thin isolating barrier, and large electric fields, resulting in significantly improved overlaps between the wave functions of the localized electrons and the heavy holes, similar to type-II InGaN/GaNAs QWs.¹³ For the higher-energy transition peak, electrons are localized in the AlN barrier and holes are localized in the GaN wells. Since AlN layers are under tensile stress, their band gaps are significantly reduced. Therefore, the PL peak at 5.061 eV could also originate from the recombination of electrons and holes being located at each of the 1 nm AlN barriers.

As the sample temperature is increased from 4.2 to 300 K, the integrated PL intensity for the 5.061 eV peak is decreased by a factor of 16 whereas that for the 3.938 eV peak is decreased only by a factor of 1.8, see Fig. 3(a). Using $I = I_0/[1 + C \exp(-E_a/kT)]$ to fit the 5.061 eV peak, the activation energy, E_a , is obtained as 18 meV. Such a value implies that the 5.061 eV transition peak can only maintain a small amount of its original strength at room temperature, as illustrated by Fig. 3(a). However, within 4.2–100 K, the ratio of the PL intensities for the two peaks is slightly increased, see Fig. 3(b), which implies that most of the localized electrons inside the AlN coupling layer move back to the GaN QWs by thermal ionization when the temperature is higher than 100 K. The ratio of the PL intensities illustrated by Fig. 3(b) is higher before the PL passes through the 10 nm GaN cap layer, due to a significantly higher absorption coefficient of the cap layer at the higher photon energy. Due to the relocation, the PL intensity at 3.938 eV is expected to increase. In addition, the conduction band edges for the GaN QWs become flattened since accumulated electron charges inside the QWs will screen the internal field. Therefore, the overlap of the wave functions of the electrons and heavy holes located inside the QWs is increased. These two factors have compensated for the significant decrease in the PL intensity. The flattened band edges cause the transition peak at 3.938 eV to blueshift, see Fig. 3(c). In contrast, the transition peak at 5.061 eV is redshifted, see Fig. 3(c), which is due to band gap reduction in AlN when increasing temperature. However, above 220 K and 280 K, the two transition peaks at 5.061 eV and 3.938 eV are blueshifted and redshifted, respectively, which could be attributed to the increasing probability for the electrons to be scattered to the bound

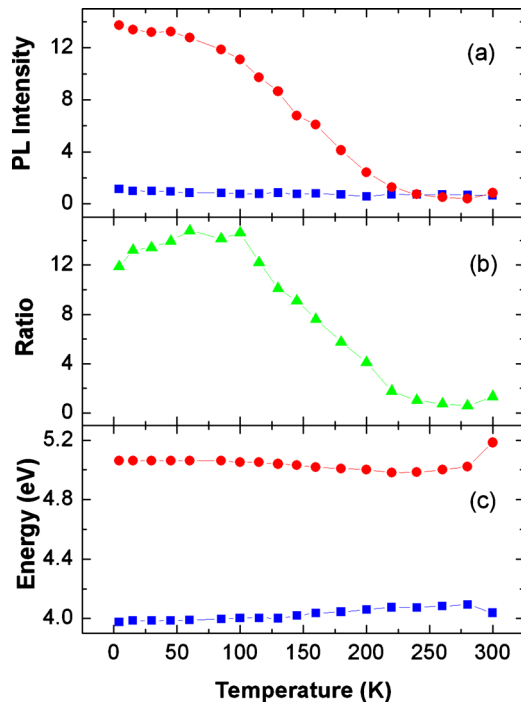


FIG. 3. (Color online) (a) Integrated PL intensities for two transition peaks of sample no. 1 vs temperature under pump power of 1.5 mW at 235 nm. Dots and the squares correspond to data and for P_{high} and P_{low} , respectively; (b) ratio of PL intensities determined from Fig. 2(a) vs temperature; and (c) transition energies of two PL peaks vs temperature.

states inside each coupling barrier by the phonons following the absorption of the pump beam.

In summary, we have observed deep ultraviolet PL peaks with their energies as high as 5.061 eV, which are attributed to the recombination of electrons in the AlN coupling barrier

with heavy holes in the GaN QWs. Compared with the single QW, the PL intensity is enhanced by two orders of magnitude. When the sample temperature is increased, PL quenching is observed due to the relocation of electrons from the AlN coupling layer to the GaN QWs.

This work has been supported by DARPA and U.S. National Science Foundation (ECCS Grant No. 0701421).

¹S. Nakamura, M. Senoh, S. Nagahama, N. Iwasa, T. Yamada, T. Matushita, H. Kiyoku, and Y. Sugimoto, *Jpn. J. Appl. Phys., Part 2* **35**, L74 (1996).

²M. Furis, A. N. Cartwright, H. Wu, and W. J. Schaff, *Appl. Phys. Lett.* **83**, 3486 (2003).

³C. Gmachl, H. M. Ng, S. N. G. Chu, and A. Y. Cho, *Appl. Phys. Lett.* **77**, 3722 (2000).

⁴D. Hofstetter, S.-S. Schad, H. Wu, W. J. Schaff, and L. F. Eastman, *Appl. Phys. Lett.* **83**, 572 (2003).

⁵H. Zhao, R. A. Arif, and N. Tansu, *IEEE J. Sel. Top. Quantum Electron.* **15**, 1104 (2009).

⁶L. Nevou, M. Tcherycheva, F. Julien, M. Raybaut, A. Godard, E. Rosencher, F. Guillot, and E. Monroy, *Appl. Phys. Lett.* **89**, 151101 (2006).

⁷A. Vardi, G. Bahir, F. Guillot, C. Bougerol, E. Monroy, S. E. Schacham, M. Tcherycheva, and F. H. Julien, *Appl. Phys. Lett.* **92**, 011112 (2008).

⁸L. Zhou, R. Chandrasekaran, T. D. Moustakas, and D. J. Smith, *J. Cryst. Growth* **310**, 2981 (2008).

⁹L. Nevou, N. Kheirodin, M. Tcherycheva, L. Meignien, P. Crozat, A. Lupu, E. Warde, F. H. Julien, G. Pozzovivo, S. Golka, G. Strasser, F. Guillot, E. Monroy, T. Remmele, and M. Albrecht, *Appl. Phys. Lett.* **90**, 223511 (2007).

¹⁰Y. K. Ee, J. M. Biser, W. Cao, H. M. Chan, R. P. Vinci, and N. Tansu, *IEEE J. Sel. Top. Quantum Electron.* **15**, 1066 (2009).

¹¹The NEXTNANO3 software is available online via <http://www.nextnano.de>.

¹²A. Vardi, N. Akopian, G. Bahir, L. Doyennette, M. Tcherycheva, L. Nevou, F. H. Julien, F. Guillot, and E. Monroy, *Appl. Phys. Lett.* **88**, 143101 (2006).

¹³R. A. Arif, H. Zhao, and N. Tansu, *Appl. Phys. Lett.* **92**, 011104 (2008).